Published in final edited form as:

Transl Res. 2018 September ; 199: 39–51. doi:10.1016/j.trsl.2018.04.005.

G-protein coupled estrogen receptor (GPER) deficiency induces cardiac remodeling through oxidative stress

Hao Wang[a,b], **Xuming Sun**[a], **Marina S. Lin**[a], **Carlos M. Ferrario**[c,d], **Holly Van Remmen**[e,f], and **Leanne Groban**[a,b]

[a]Department of Anesthesiology, Wake Forest School of Medicine, Medical Center Boulevard, Winston Salem, North Carolina, 27157 USA

[b]Department of Internal Medicine-Molecular Medicine, Wake Forest School of Medicine, Medical Center Boulevard, Winston Salem, North Carolina, 27157 USA

[c]Department of Surgery, Wake Forest School of Medicine, Medical Center Boulevard, Winston Salem, North Carolina, 27157 USA

[d]Department of Physiology and Pharmacology, Wake Forest School of Medicine, Medical Center Boulevard, Winston Salem, North Carolina, 27157 USA

[e]Aging and Metabolism Research Program, Oklahoma Medical Research Foundation, 825 N.E. 13th Street, Oklahoma City, OK, 73104 USA

[f]Oklahoma City VA Healthcare System, 921 N.E. 13th Street, Oklahoma City, OK 73104 USA

Abstract

Oxidative stress has been implicated in the unfavorable changes in cardiac function and remodeling that occur after ovarian estrogen loss. Using ovariectomized (OVX) rat models, we previously reported that the cardioprotective actions of estrogen are mediated by the G-protein coupled estrogen receptor (GPER). Here, in 9-month-old, female cardiomyocyte-specific GPER knockout (KO) mice vs. sex- and age-matched wild type (WT) mice, we found increased cardiac oxidative stress and oxidant damage, measured as a decreased ratio of reduced glutathione to oxidized glutathione (GSH/GSSG), increased 4-hydroxynonenal (HNE) and 8-hydroxy-2′-deoxyguanosine (8-oxo-DG) staining, and increased expression of oxidative stress-related genes. GPER KO mice also displayed increased heart weight, cardiac collagen deposition, and Doppler-derived filling pressure (E/e′), and decreased percent fractional shortening and early mitral annular

Corresponding Author: Leanne Groban, MD, Department of Anesthesiology, Wake Forest School of Medicine, Medical Center Boulevard, Winston Salem, NC 27157-1009, Ph: +1 336-716-4498, Fax: +1 336-716-8190, lgroban@wakehealth.edu.

Declaration of interest

The authors declare that there are no competing interests associated with the manuscript.

Author contribution statement

HW and LG participated in research design. HW, XS, ML, HVR, and LG conducted experiments. HW, XS, and LG performed data analysis and formatting of figures. LG wrote the first draft of the manuscript, with contributions from HW and CMF. All authors contributed and approved the final version of the manuscript.

velocity (e′) compared to WT controls. Treatment of GPER KO mice for 8 weeks with MitoQ, a mitochondria-targeted antioxidant, significantly attenuated these measures of cardiac dysfunction, and MitoQ decreased 8-oxo-DG intensity compared to treatment with an inactive comparator compound dTPP ($P < 0.05$). A real-time PCR array analysis of 84 oxidative stress and antioxidant defense genes revealed that MitoQ attenuates the increase in Nox4 and Ptgs2 and decrease in Ucp3 and Gstk1 seen in GPER KO mice. Our findings suggest that the cardioprotective effects of GPER include an antioxidant role and that targeted strategies to limit oxidative stress after early noncancerous surgical extirpation of ovaries or menopause may help limit alterations in cardiac structure and function related to estrogen loss.

Keywords

GPER; G-protein coupled estrogen receptor; ovariectomy; estrogen; reactive oxygen species; antioxidant genes; oxidative stress; left ventricular function

INTRODUCTION

Heart failure (HF) affects approximately 3 million American women[1] and its prevalence has been projected to increase by 46% by the end of 2030.[2] Of the two types of heart failure, women are more prone to the development of heart failure with preserved ejection fraction (HFpEF) than men of the same age,[3] which has been attributed, in part, to the loss of estrogenic cardioprotection. Emerging epidemiologic evidence also suggests that early menopause is positively associated with incident HF.[4,5] These trends highlight the importance of understanding the pathophysiologic alterations and molecular mechanisms that precede the development of HF in women upon loss of ovarian estrogens, particularly the development of left ventricle diastolic dysfunction (LVDD), a precursor of HFpEF.

Preclinical evidence shows that ovarian sex hormones, primarily estrogens, are involved in the preservation of cardiac function and structure in the female heart.[6–9] In various rodent models, including the normal aging Brown Norway × Fischer344 rat,[10,11] the estrogen-sensitive hypertensive mRen2.Lewis rat,[12–17] and the spontaneously hypertensive rat (SHR) and its normotensive Wistar Kyoto (WKY) counterpart,[18,19] ovariectomy (OVX) leads to LVDD and LV interstitial or hypertrophic remodeling. Treatment with 17-β estradiol reverses or prevents OVX-induced cardiac dysfunction and remodeling,[13] in part through activation of the G-protein coupled estrogen receptor, GPER.[16,20] GPER is a membrane-bound receptor that binds the active form of estrogen, estradiol (E2), with high affinity, but signals differently from the canonical ERs (ERα and ERβ). We found that GPER activation maintains cardiac structure and function after estrogen loss via anti-proliferation effects in cardiac fibroblasts[21] and mast cells, attenuation of cardiac chymase/angiotensin II expression/activity,[22] and modulation of sarcoplasmic reticulum calcium regulatory proteins[10] to limit cardiomyocyte (CM) stiffness. The successful generation of a CM-specific GPER knockout (GPER KO) mouse, which shows impaired cardiac function and increased wall thicknesses with cardiac deactivation of GPER in females, provides a model in which we can examine the exact roles of this membrane estrogen receptor in conferring cardioprotection.[23]

Increased oxidative stress after estrogen loss contributes to the development of left ventricular hypertrophy in postmenopausal women and female OVX rodent models.[24–26] An increase in mitochondrial reactive oxygen species (ROS) production, specifically hydrogen peroxide (H_2O_2), has been reported in hearts from OVX rats,[27] with ROS reverting to normal levels when OVX rats were treated with estrogen.[28] Moreover, lower heart oxidative damage has been described in gonad-intact females compared to male rats, and in aged female rats compared to their younger counterparts,[27] implicating estrogens in the regulation of mitochondrial ROS production. We hypothesize that GPER mediates the inhibitory effects of estrogen on cardiac ROS production, thereby protecting the heart against LV remodeling and dysfunction. Activation of GPER has been shown to decrease oxidative stress in rat arteries,[29] kidney tubular cells,[30] cultured cortical neurons,[31] and CM subjected to doxorubicin toxicity.[32] In the mRen2.Lewis rat heart, we showed that the GPER agonist G1 inhibits OVX-induced increases in cardiac NADPH oxidase 4 (Nox4).[16]

To limit mitochondrial oxidative damage, many mitochondria-targeted antioxidants have been developed. The most extensively studied of these is MitoQuinone (Phosphonium [10-(4,5-dimethoxy-2-methyl 3,6-dioxo-1,4-cyclohexadien-1-yl)decyl] triphenyl-, mesylate; MitoQ), which contains the antioxidant quinone moiety covalently attached to a lipophilic triphenylphosphonium cation.[33] Chronic treatment with MitoQ has been shown to protect against oxidative damage in rat and mouse models of ischemia reperfusion,[34], hypertension, [35] volume and pressure overload,[36,37] and cocaine-induced cardiac toxicity,[38] as well as in two phase 2 clinical trials.[33] The present study was designed to compare the extent of oxidative stress in hearts of female GPER KO mice versus wild-type (WT) littermates and examine the ability of MitoQ to ameliorate LV dysfunction and remodeling in GPER KO mice. We also tested the hypothesis that MitoQ treatment reduces cardiac ROS production and limits the genomic response to oxidative stress.

MATERIAL AND METHODS

Animals

CM-specific GPER KO mice were generated in our lab, as described previously.[23,39] $GPER^{f/f/Cre}$ (GPER KO) and $GPER^{f/f}$ littermates (GPER WT) were studied at 7–9 months of age in 2 separate cohorts. In the first cohort, oxidative stress was assessed in the hearts from untreated GPER KO and WT mice (n = 4–5/group, 9 months of age). In the second cohort, mice received chronic treatment with MitoQ or its inactive comparison compound decylTPP (dTPP), as described in detail below. All mice were housed in a facility approved by the Association for Assessment and Accreditation of Laboratory Animal Care, with a 12-h light/dark cycle and constant temperature and humidity. Mice had ad libitum access to standard chow (Nestle Purina, St. Louis, MO) and tap water. Body weight and water intake were monitored regularly throughout the study. At the time of sacrifice, mice were administered pentobarbital sodium (Akorn Inc., Lake Forest, IL; 100 mg/kg body weight) by i.p. injection. Upon verification of deep anesthesia by the absence of response to tail/toe pinches, the chest was opened and the heart was quickly excised and trimmed. Whole heart and LV weight were measured and normalized to body weight. The LV was sectioned transversely from base to apex and fragments were either snap frozen in liquid nitrogen and

stored at −80°C in cryogenic tubes for RNA extraction or fixed in 4% formaldehyde for paraffin-embedded sectioning. All procedures were carried out in accordance with the Guide for the Care and Use of Laboratory Animals, published by National Institute of Health, and study approval was obtained from the Animal Care and Use Committee of Wake Forest University (protocol # A15-191).

HNE and 8-oxo-DG staining for ROS production

Paraffin-embedded LV sections (5 μm) were prepared for assessment of oxidative modification of cell injury. The presence of 4-hydroxynonenal (4-HNE), representing lipid peroxide, was assessed by diaminobenzidine (DAB) staining with rabbit polyclonal anti-HNE antibody (Alpha Diagnostic International, San Antonio, TX) at 1:500 dilution. Oxidative stress-induced DNA damage was measured by the presence of 8-hydroxy-2′-deoxyguanosine (8-oxo-DG) with mouse monoclonal anti-8-oxo-DG at 1:200 dilution (Rockland Immunochemicals Inc., Limerick, PA), as described previously by others.[40,41]

Redox status (GSH/GSSG ratio) determination

Reduced glutathione (GSH) is one of the main scavengers of ROS, and its ratio to oxidized glutathione (GSSG) is used as a marker of oxidative stress.[42,43] Flash frozen cardiac tissue samples were prepared for analysis of GSH and GSSG by extraction with 5% meta-phosphoric acid. Using 1 pmol in 1 μg and 25 μg tissue for GSH and GSSG, respectively, metabolites were resolved by reverse phase ion pairing HPLC and detected and quantified using electrochemical analysis, as previously described.[44]

Real-time quantitative PCR analysis of oxidative stress-related gene expression

Oxidative stress-related genes Nox4, Ptgs2, GPX1, Sirt3, Ucp3, and Gstk1 were selected based on the literature, our previous studies, and previous microarray data from CM of GPER KO mice.[23] qPCR was used to detect mRNA levels in the LV as previously described.[16,23] Total RNA was extracted from LV tissue using the RNeasy Lipid Tissue Mini Kit (Qiagen, Inc., Germantown, MD) and further purified using RNeasy MinElute Cleanup Kit (Qiagen, Inc.) followed by quality assessment on an agarose gel. Complementary first-strand DNA was synthesized using the Omniscript RT kit (Qiagen Inc.). Relative quantification of mRNA levels by qPCR was performed using a SYBR Green PCR kit (Qiagen Inc.). Amplification and detection were performed with the QuantStudio 3 Real-Time PCR system (Applied Biosystems, Foster City, CA). Sequence-specific oligonucleotide primers were designed according to published GenBank sequences and confirmed with OligoAnalyzer 3.0. The sequences of the primers used are listed in Supplementary Table 1. The relative target mRNA levels in each sample were normalized to glyceraldehyde 3-phosphate dehydrogenase (GAPDH). Expression levels are reported relative to the mean value of the control group.

Animal treatment

MitoQ is comprised of the antioxidant ubiquinone (CoQ10) linked to (1-Decyl) triphenylphosphonium bromide (dTPP). dTPP is lipophilic, thereby facilitating the movement of MitoQ across the cell membrane and accumulation within the mitochondrial

matrix, in response to the membrane potential.[45,46] Inside the mitochondria, scavenging ROS is achieved through oxidation of MitoQ into its quinone form, which is then recycled back into the active ubiquinol form via action of complex II.[47] In a separate cohort, mice at 7 months of age were randomly assigned to treatment in drinking water with either MitoQ (500 μmol/L; kindly donated by MitoQ Ltd, Auckland, New Zealand) (GPER KO MitoQ-treated mice, $n = 9$; WT MitoQ-treated mice, $n = 7$] or the inactive comparison compound dTPP (500 μmol/L) (GPER KO dTPP-treated mice, $n = 7$; WT dTPP-treated mice, $n = 7$) for 8 weeks. This dose of MitoQ was chosen as no evidence of toxicity was found when 500 μmol/L was administered to mice in their drinking water for 28 weeks.[48] MitoQ (MitoQ Ltd., Auckland, New Zealand) and dTPP (MedKoo Biosciences, Morrisville, NC) were prepared fresh every third day, protected from light, and stored at 4°C. While all cardiomyocyte-specific GPER KO mice reach adulthood with no obvious phenotype (*e.g.*, exercise tolerance is unaffected at 15 weeks of age),[23] they have a decreased lifespan of ~9–10 months due to cardiac failure. After 7 months of age, mutant female mice begin showing consistent echocardiographic signs of left ventricular dilation; thus, we chose to begin the 8-week MitoQ or dTPP treatment at 7 months of age.

In vivo experimental procedures

After 8 weeks of treatment with either MitoQ or dTPP, systolic blood pressure (SBP) was measured by tail-cuff in conscious restrained mice using the CODA 6 system (Kent Scientific Corp, Torrington, CT), as described previously.[23] LV morphometrics and function were determined at the end of the 8-week treatment protocol using a commercially available echocardiograph equipped with both PureWave 12-4 MHz sector and 15-7 MHz linear transducers (CX50 CompactXtreme System; Philips Medical Systems) by the same investigator (LG), who was masked to the experimental groups. In brief, mice were anesthetized with an isoflurane (1.5%) oxygen mixture by nose cone and secured in the supine position to a warm (37.5°C) imaging platform. A commercially available paw sensor (PhysioSuite Monitor, Kent Scientific Corp) was applied for continuous pulse oximetry and heart rate monitoring to gauge the depth of anesthesia and to maintain the animals' safety throughout the procedure. The 15 MHz linear probe was used to obtain 2D-guided, LV M-mode images in the short-axis parasternal view using LV end diastolic and end systolic dimensions (LVEDD and LVESD) and posterior and anterior wall thicknesses (PWTed and AWTed) at end diastole. The 12 MHz phased array probe was used to obtain the apical four-chamber view for transmitral inflow Doppler (early transmitral filling or maximum E-wave velocity) and septal tissue Doppler measurements (early mitral annular descent or e′) of diastolic function. Heart rate was determined from 5 consecutive RR intervals from pulsed-Doppler inflow tracings. The fractional shortening (FS) of the LV was expressed as %FS = (LVEDD-LVESD)/LVEDD × 100. The relative wall thickness (RWT) was calculated as (PWTed + AWTed)/LVEDD. The early mitral inflow filling velocity-to-early mitral annular velocity ratio, or E/e′, was used to estimate LV filling pressure and the extent of diastolic dysfunction.

Heart tissue collection and preparation

After 8 weeks of treatment, hearts were collected and LV tissue was prepared for RNA extraction and paraffin-embedded sectioning, as described above.

Histochemical analysis

For histological analysis, paraformaldehyde-fixed and paraffin-embedded LV specimens were cut into 5 μm sections and collagen was stained with picrosirius red, as previously described.[14,19] Images were captured using a Nikon Eclipse TE300 Inverted Fluorescence Microscope (Spach Optics Inc., Pittsford, NY). The ratio of collagen-stained pixels to unstained pixels was quantified using NIH ImageJ software (http://rsbweb.nih.gov/ij/). Four animals in each group were used for analysis.

Real-time PCR microarray analysis

Total RNA isolation and cDNA synthesis were performed as described above for real-time qPCR analysis. Real-time PCR microarray analysis was performed using the mouse oxidative stress and antioxidant defense array kit (Cat. no. PAMM-065, SuperArray Bioscience, Frederick, MD), focusing on gene families relevant to the induction and inhibition of ROS production and genes involved in ROS metabolism. The selected 84 gene set included 3 reverse transcription controls and 3 positive PCR controls, a genomic contamination control, and 5 constitutively expressed housekeeping genes. The assay used a RT2 SYBR Green/Rox PCR master mix (Cat. no. PA-012, SuperArray Bioscience) on a QuantStudio 3 Real-Time PCR system (Applied Biosystems). The integrated web-based software package for the PCR array system automatically performed all comparative threshold cycle ($\Delta\Delta C_t$)–based fold-change calculations from the uploaded data. For these calculations, C_t values were normalized based on an automatic selection from a full panel of reference genes. Three mice per group were used for this analysis. A two-fold or greater change in expression with $P \leq 0.05$ was considered significant.

Statistical analyses

All results are expressed as mean ± SEM. Data obtained from cohort 1 (WT vs. KO) and PCR microarray were analyzed using a two-tailed Student's *t*-test assuming equal variance. Data obtained from echocardiography, tail-cuff blood pressure, immunoblot, and histopathology involving cohort 2 were evaluated by two-way ANOVA to determine the effect of genotype (KO vs. WT), treatment (MitoQ vs. dTPP), and genotype x treatment followed by a post-*hoc* Newman-Kuels multiple comparison test. Data were analyzed using the software GraphPad Prism Version 6 (GraphPad Software, Inc., La Jolla, CA). $P < 0.05$ was considered statistically significant.

Results

GPER KO mice show elevated cardiac oxidative stress

Evidence for increased cardiac oxidative stress in GPER KO versus WT mice from cohort 1 was determined by immunohistological and biochemical methods. Assessment of oxidative modification of cell injury using markers of lipid and DNA damage with 4-HNE and 8-oxo-DG, respectively, showed greater damage in hearts from GPER KO mice compared to WT mice (Figure 1A). Although cardiac GSH levels in WT and GPER KO mice were not different, GSSG was significantly higher in GPER KO mice and thus the GSH/GSSG ratio was lower compared to WT mice (Figure 1B). Cardiac mRNA levels of the oxidative stress-

related genes Nox4, Pgts2, and Gpx1 were increased in GPER KO mice by 4-, 4-, and 1.8-fold, respectively, while the antioxidant defense genes Sirt3, Ucp3, and Gstk1 were decreased by 1.8-, 3.4-, and 2.4-fold, respectively, compared to WT mice ($P < 0.05$) (Figure 1C).

MitoQ improves GPER KO-related declines in LV systolic and diastolic function

Eight weeks of treatment with MitoQ or dTPP did not affect the activity of the GPER KO or WT mice in cohort 2. Neither genotype nor treatment had an effect on body weight or SBP (Table 1). There were statistically significant interactions between the effects of genotype and treatment on %FS [$F(1, 26) = 4.665$, $P = 0.041$], e' [$F(1,26) = 6.650$, $P = 0.016$], and E/e' [$F(1,26) = 7.335$, $P = 0.0123$]. Specifically, GPER KO mice treated with MitoQ exhibited significant improvements in FS, e', and E/e' compared to GPER KO mice treated with dTPP ($P < 0.05$), whereas in WT mice, no differences with respect to treatment were observed (Figure 2). Consistent with previous reports,[23] these indices of systolic and diastolic function, including early deceleration time (Table 1) were significantly impaired in GPER KO mice treated with dTPP compared to WT mice treated with dTPP (genotype effect: $P < 0.001$ for FS, e', and E/e'). Doppler-derived heart rate, transmitral early filling velocity, and M-mode indices of LV chamber and wall dimensions were not significantly affected by genotype or treatment (Table 1).

MitoQ decreases heart weight and cardiac collagen deposition in GPER KO mice

MitoQ treatment significantly reduced heart weight-to-body weight in GPER KO mice compared to dTPP-treated GPER KO mice (treatment effect: $F(1,26) = 6.52$, $P = 0.016$) (Figure 3A). There was a statistically significant interaction between the effects of genotype and treatment on collagen deposition ($F(1,12) = 15.14$, $P = 0.002$). Notably, this marker of interstitial fibrosis was significantly increased in LV sections of dTPP-treated GPER KO mice compared to either MitoQ-treated GPER KO mice or WT littermates treated with either dTPP or MitoQ (Figures 3B and 3C). Even though MitoQ attenuated the extent of fibrosis in KO hearts, the volume of collagen remained significantly greater when compared to WT hearts, irrespective of treatment.

MitoQ decreases 8-oxo-DG, but not 4-HNE, in the LV of GPER KO mice

Consistent with our findings from cohort 1, there were significant effects of genotype on both 8-oxo-DG ($F(1,12) = 114$, $P < 0.0001$) and 4-HNE ($F(1,12) = 51.80$, $P < 0.0001$). ROS staining in GPER KO hearts, irrespective of treatment, was substantially enhanced compared to that in WT-dTPP or WT-MitoQ hearts (Figure 4A,B and 4C,D). MitoQ treatment had a significant impact on cardiac DNA damage, as demonstrated by attenuated 8-oxo-DG staining (treatment effect: $F(1,12) = 13.20$, $P = 0.003$), particularly in GPER KO hearts ($P < 0.01$; Figure 4B). An interaction between genotype and treatment accounted for about 3% of the total variance in this index of cardiac ROS (interaction effect: $P = 0.058$). Lipid peroxidation, as evidenced by 4-HNE staining intensity, was not affected by MitoQ.

MitoQ ameliorates the effect of GPER KO on oxidative stress-related gene expression

Of the 84 oxidative stress and antioxidant defense genes tested, 10 were differentially expressed in dTPP-treated GPER KO mice compared to dTPP-treated WT littermates (8 overexpressed and 2 underexpressed). Genes that were significantly upregulated in GPER KO mice treated with dTPP included Nox4, prostaglandin-endoperoxide synthase 2 (Ptgs2), chemokine (C-C motif) ligand 5 (Ccl5), apolipoprotein E (apoE), stearoyl-coenzyme A desaturase 1 (Scd1), vimentin (Vim), neutrophil cytosolic factor 2 (Ncf2), serine (or cysteine) peptidase inhibitor b1b (Serpinb1). Genes significantly downregulated in GPER KO mice treated with dTPP mice included uncoupling protein 3 (Ucp3) and glutathione S-transferase kappa 1 (Gstk1) (Figure 5A; Supplementary Figure 1A and Table 2). Glutathione peroxidases (Gpx) 1, 4, and 5 were decreased up to 4-fold; however, these values did not meet the threshold for significance (Figure 5A, Supplementary Figure 1A and Table 2).

Of the 84 genes, 4 were significantly upregulated in MitoQ-treated GPER KO mice compared to dTPP-treated WT mice, including Ccl5, neutrophil cytosolic factor 1 (Ncf1), apoE, and Scd1, while no genes met the criteria of downregulation (Figure 5B; Supplementary Figure 1B and Table 2). MitoQ treatment attenuated the fold change in gene expression by 10% to 50% for the 8 genes that were upregulated in GPER KO mice treated with dTPP.

Discussion

The main findings in this study are: 1) 7-month old female GPER KO mice exhibit increased cardiac oxidative stress when compared to WT littermates, which can be linked to the LV dysfunction and remodeling already established in this new genetically modified model[23] and 2) the mitochondria-targeted antioxidant MitoQ limits LV dysfunction and modulates oxidative stress in hearts of GPER KO mice.

GPER in vascular and renal cells has an important role in blood pressure regulation;[49] however, the present data and our previous findings suggest that cardiac-specific GPER deletion has no effect on systolic blood pressure.[23] Although MitoQ might reduce blood pressure in hypertensive models,[50,51] its administration in the drinking water of GPER KO mice did not overtly lower tail cuff blood pressure, which is consistent with findings in an aged normotensive mouse model.[52] Indeed, it is possible that use of more invasive measurements may uncover systemic effects of this mitochondria-targeted antioxidant. Taken together, our results suggest that the consequence of cardiac GPER deletion or MitoQ treatment on oxidative stress and cardiac performance are largely independent of peripheral actions.

The decline and cessation of estrogen production from reproductive aging or surgery has been linked to increases in oxidative stress[25,53] and cardiovascular disease risk.[54–56] Preclinical studies from our laboratory have shown that chronic activation of GPER confers cardioprotection from remodeling and LVDD in female rodent hearts induced by 1) high salt,[57] 2) OVX-associated exacerbations in systemic and pulmonary arterial hypertension, and 3) normal aging, without eliciting a uterotrophic response.[10,16,58] As this is an important distinction from the unfavorable side effects seen in classic ER agonism with

postmenopausal hormone replacement therapy,[59,60] GPER becomes an appealing target for enhancing the cardiac structural and lusitropic benefits of estrogen. To determine the exact roles of GPER in the heart and to emulate GPER inactivation that occurs upon estrogen loss, we developed the CM-specific GPER KO mouse, which shows significant evidence of LV remodeling and heart failure. As an extension of our previous work,[23] this study showed that LV dysfunction and hypertrophy in GPER KO arises with concomitant increases in cardiac ROS production and oxidative stress, as evidenced by increases in 8-oxo-DG staining and reductions in the GSH/GSSG ratio. Immunohistochemical evidence of increased ROS in GPER KO mice was attenuated by treatment with MitoQ. In addition, MitoQ attenuated the genomic response to oxidative stress and enhanced gene expression levels to antioxidant defense from cardiac GPER deficiency, suggesting a critical linkage of oxidative stress to cardiac GPER deactivation that occurs with estrogen loss.

MitoQ is the most highly studied antioxidant and has been shown to protect against cardiac function loss, as well as tissue and mitochondrial damage, in response to ischemia reperfusion,[34] hypertension,[35] volume overload,[36] and cocaine-induced cardiac toxicity,[38] in experimental animal models. In our study, MitoQ treatment decreased biomarkers of lipid peroxidation and DNA oxidation in KO hearts, indicating that mitochondrial ROS production contributes to the pathogenesis of LV dysfunction in the GPER KO mouse model.[23] This is further supported by the relative reduction in many oxidative metabolism response genes, and increase in antioxidant genes, compared to GPER KO mice treated with the inactive lipophilic dTPP compound.

Our results suggest that estrogen-mediated mitochondrial-antioxidant actions occur through GPER. Bopassa et al.[61] previously showed that G1 inhibits mitochondrial permeability transition pore opening in mouse hearts subjected to ischemia-reperfusion injury and Sbert-Roig et al.[62] recently showed that in H9c2 cardiomyocytes, G1 mimics the effects of E2 in enhancing mitochondrial biogenesis, which can be blocked by the GPER antagonist G15. Our findings that MitoQ limits the extent of LV remodeling, measures of heart failure, and oxidative damage in GPER KO hearts support an antioxidant defense role for cardiac GPER.

An imbalance between the production of ROS and the detoxification of reactive intermediates, such as peroxides and free radicals, can be damaging to proteins, lipids, and nucleic acids, increasing local oxidative stress. Indeed, mitochondrial dysfunction leading to ROS accumulation is among the emerging CM-centric targets for the treatment of HFpEF[63] and cellular targets for other female sex-specific pathologies. Despite growing interest in the role of oxidant stress in progression of female sex-specific heart disease, the estrogen receptors and pathways that contribute to oxidative damage in the estrogen-deficient cardiovascular system remain unclear. Steagall et al.[64] recently showed an ERα-dependent restoration of catalase and superoxide dismutase activities and reduction of ROS in the myocardium of OVX rats, while selective ERβ or GPER activation produced opposite effects. A study by Kararigas et al.[65] using the ERβ KO mouse found that ERβ was necessary for the decrease in expression of cardiac genes involved in oxidative phosphorylation in response to pressure overload. In vascular tissue, the two classical ER subtypes differentially regulate genes involved in ROS production, with the ERβ pathway reducing expression of ROS-generating activities (*e.g.*, electron transport complex subunits),

and the ERα pathway enhancing gene expression within antioxidant systems and reducing expression of genes involved in in ROS-generating processes.[66] Intriguingly, whole-body genetic deletion of GPER in mice reduced oxidative stress to slow vascular aging in mice by reducing NADPH oxidase expression,[67] whereas selective GPER activation with its agonist G1 attenuated salt-induced aortic remodeling in part by reducing oxidative stress in gonad-intact hypertensive mRen2.Lewis rats.[29] Our PCR array analysis identified distinct transcriptional profiles of several key genes and gene families involved in oxidative stress and antioxidant defense in the female GPER KO mouse heart that correlate with LV dysfunction and hypertrophy.

Nox4 was the most significantly upregulated gene identified by the PCR array, with a 12-fold increase in expression in the GPER KO vs. WT heart. Nox4 is a member of a flavoenzyme family that reduces molecular oxygen to superoxide, which can be further converted to H_2O_2. Additional genes involved in superoxide metabolism, Scd1 and Ncf2, were upregulated in the hearts of GPER KO compared to WT mice. Scd1, a key enzyme in fatty acid metabolism, has been implicated in the modulation of cell inflammation and stress[68] while Ncf2 encodes a cytosolic protein that is a component of the NADPH oxidase complex. Ptgs2, also known as cyclooxygenase 2, was overexpressed 6-fold in GPER KO vs. WT mice. It is a key enzyme in prostaglandin biosynthesis, functioning both as a dioxygenase and as a peroxidase, and has been shown to play a role in inflammatory processes associated with cardiac hypertrophy and heart failure.[69] Ccl5 was also significantly upregulated in GPER KO hearts; chemokine Ccl5/RANTES (Regulated on Activation Normal T cell Expressed and Secreted) is involved in the recruitment of several inflammatory cell subsets to inflammatory sites, including monocytes, neutrophils, dendritic cells, and lymphocytes.[70] Oxidant stress-mediated enhancement of gene expression of apoE may reflect an attempt to counteract inflammation in the GPER KO model. Moreover, upregulation of Serpinb1 in GPER KO hearts could signify a defense mechanism against cellular damage. Serpinb1 encodes EIA in mice, which inhibits neutrophil elastases, cathepsin G, proteinase-3, and chymotrypsin, similar to that of the human gene MNEI (monocyte neutrophil elastase inhibitor). Taken together, these data support a generalized higher level of oxidative stress in the hearts of GPER KO mice.

In addition to genomic alterations among key ROS producers, we detected downregulation of genes specific to cellular antioxidant defense in GPER KO hearts: Gstk1 and Ucp3. Gstk1 encodes a member of the kappa class of the glutathione transferase superfamily of enzymes, which function in cellular detoxification and are localized in mitochondria and peroxisomes. Downregulation of Gstk1 has recently been linked to hypertrophic cardiomyopathy,[71] which may be relevant in terms of the oxidative stress, lipid peroxidation, and LV dysfunction observed in GPER KO hearts. The downregulation of Ucp3 could have important implications for protection against ROS-induced cellular damage. Normally, activation of Ucp3 leads to mild uncoupling that aids in lowering the proton-motive force across the inner mitochondrial membrane, thereby attenuating mitochondrial production of free radicals and protecting against oxidative damage.[72]

In addition to changes in expression of Ucp3, we observed a modest, yet significant, 1.6-fold downregulation in the gene encoding superoxide dismutase 2 (Sod2) (see Supplemental

Table 2). This is an important mitochondrial antioxidant enzyme that catalyzes the dismutation or partition of superoxide anions produced by the respiratory chain into H_2O_2, which is then catalyzed to H_2O by catalase, peroxiredoxins (Prxs), or glutathione peroxidases (Gpx). Downregulation of Sod2 in GPER KO hearts suggests impaired antioxidant defense, leading to increased oxidative stress that may cause oxidative damage and LV dysfunction. Except for Gpx7, the majority of genes in the glutathione peroxidase family, which encode enzymes that catalyze the reduction of H_2O_2 and organic hydroperoxides, were not consistently affected by the loss of GPER. Gpx7, however, was significantly upregulated 1.9-fold in GPER KO mice, suggesting a compensatory response triggered by the increased cardiac ROS. Taken together, the changes observed in oxidative response and antioxidant defense genes in hearts of GPER deficient mice support a potential role for GPER in the maintenance of local redox balance. The molecular mechanisms responsible for GPER deficiency-associated gene changes in oxidative metabolism and defense are not clear, but given that the actions of GPER are primarily nongenomic,[73,74] it is likely these effects are secondary to LV functional derangements due to GPER KO rather than a direct effect on gene transcription.

The clinical implications of this study are important considering that the underlying etiology of female sex-specific heart disease, and specifically heart failure, remains unclear and there are no proven pharmacotherapies to halt disease progression after natural or surgically induced cessation of ovarian hormone production. Based on the present findings, MitoQ or other mitochondria-targeted antioxidants might be a potential treatment to offset estrogen loss and GPER deactivation-related heart disease in postmenopausal women. However, we also realize the limitations of this study. Although we demonstrated that cardiomyocyte GPER deletion impairs heart structure and function, and that these effects can be attenuated by MitoQ, it remains to be determined whether GPER activation alone or in combination with MitoQ might have equal or even more advantageous antioxidant effects in this model. Also, ROS itself can act as a subcellular messenger in gene regulatory and signal transduction pathways. Oxidative stress in various cell model systems affects gene expression of ERα and ERβ differently, and their effects can be blocked by antioxidants.[75] How cardiac oxidative stress and/or MitoQ influence GPER expression and activity is not known and will require further investigation.

In summary, our data show that loss of GPER in the CM of female mice leads to increased oxidative stress, which may account for declines in LV function, interstitial remodeling, and hypertrophy. Moreover, MitoQ treatment limited the extent of oxidative damage (8-oxo-DG), modulated the genomic response to oxidative stress, suppressed collagen deposition, and improved LV systolic and diastolic function in CM-specific GPER KO mice. While the mitochondrial respiratory chain is the primary source of ROS formation, oxidative stress can also occur via xanthine oxidases, reduced nicotinamide adenine dinucleotide phosphate oxidases, and uncoupling of nitric oxide synthases. Accordingly, future studies will focus on GPER-mediated cellular and subcellular mechanisms that counterbalance aberrations in either mitochondrial function and/or antioxidant systems after ovarian estrogen loss. These studies may reveal new targets for cardiac-specific therapeutics to limit oxidative stress and slow the progression of LVDD and the development of left ventricular hypertrophy in aging women.

Supplementary Material

Refer to Web version on PubMed Central for supplementary material.

Acknowledgments

The authors would like to thank the Oklahoma Nathan Shock Center of Excellence in the Biology of Aging for their assistance in performing the GSH/GSSG cardiac redox assay. The authors would also like to acknowledge MitoQ, Ltd. for generously providing MitoQ. All authors attest that they have read the journal's Conflict of Interest policy and Authorship Agreement.

Funding information

This work was funded by grants from the National Institute on Aging of the National Institute of Health (LG) AG033727 and the National Heart Lung and Blood Institute of the National Institute of Health (CMF and LG P01-HL051952). Dr. Van Remmen is supported by a Senior Research Scientist Career award from the Department of Veterans Affairs.

Abbreviations

4-HNE	4 hydroxynonenal
apoE	apolipoprotein E
AWTed	anterior wall thickness at end diastole
C-C motif	chemokine
Ccl5	ligand 5
CoQ10	ubiquinone
DAB	diaminobenzidine
FS	fractional shortening
GAPDH	glyceraldehyde 3-phosphate dehydrogenase
Gpx	glutathione peroxidases
Gstk1	glutathione S-transferase kappa 1
HPLC	High-performance liquid chromatography
LVEDD	left ventricular end diastolic dimension
LVESD	left ventricular end systolic dimension
MitoQ	Phosphonium [10-(4,5-dimethoxy-2-methyl 3,6-dioxo-1,4-cyclohexadien-1-yl)decyl] triphenyl-, mesylate
NADPH	Dihydronicotinamide-adenine dinucleotide phosphate
Ncf1	neutrophil cytosolic factor 1
Ncf2	neutrophil cytosolic factor 2

Nox4	NADPH oxidase 4
Prxs	peroxiredoxins
Ptgs2	prostaglandin-endoperoxide synthase 2
PWTed	posterior wall thickness at end diastole
RNA	ribonucleic acid
ROS	reactive oxygen species
RWT	relative wall thickness
SBP	systolic blood pressure
Scd1	stearoyl-coenzyme A desaturase 1
Serpinb1	serine (or cysteine) peptidase inhibitor b1b
Sod2	superoxide dismutase 2
Ucp3	uncoupling protein 3
Vim	vimentin

References

1. Mozaffarian D, Benjamin EJ, Go AS, et al. Executive summary: Heart disease and stroke statistics —2016 update. Circulation. 2016; 133:447–454. [PubMed: 26811276]
2. Heidenreich PA, Albert NM, Allen LA, et al. Forecasting the impact of heart failure in the United States: a policy statement from the American Heart Association. Circ Heart Fail. 2013; 6:606–619. [PubMed: 23616602]
3. Hogg K, Swedberg K, McMurray J. Heart failure with preserved left ventricular systolic function; epidemiology, clinical characteristics, and prognosis. J Am Coll Cardiol. 2004; 43:317–327. [PubMed: 15013109]
4. Appiah D, Schreiner PJ, Demerath EW, Loehr LR, Chang PP, Folsom AR. Association of age at menopause with incident heart failure: A prospective cohort study and meta-analysis. J Am Heart Assoc. 2016; 5:e003769. [PubMed: 27468929]
5. Ebong IA, Watson KE, Goff DC, et al. Age at menopause and incident heart failure. Menopause. 2014; 21:585–591. [PubMed: 24423934]
6. Li S, Gupte AA. The role of estrogen in cardiac metabolism and diastolic function. Methodist Debakey Cardiovasc J. 2017; 13:4–8. [PubMed: 28413575]
7. Iorga A, Li J, Sharma S, et al. Rescue of pressure overload-induced heart failure by estrogen therapy. J Am Heart Assoc. 2016; :5. pii: e002482. doi: 10.1161/JAHA.115.002482
8. Chen Y, Zhang Z, Hu F, et al. 17β-estradiol prevents cardiac diastolic dysfunction by stimulating mitochondrial function: a preclinical study in a mouse model of a human hypertrophic cardiomyopathy mutation. J Steroid Biochem Mol Biol. 2015; 147:92–102. [PubMed: 25541436]
9. Zhao Z, Wang H, Jessup JA, Lindsey SH, Chappell MC, Groban L. Role of estrogen in diastolic dysfunction. Am J Physiol Heart Circ Physiol. 2014; 306:H628–H640. [PubMed: 24414072]
10. Alencar AK, da Silva JS, Lin M, et al. Effect of age, estrogen status, and late-life GPER activation on cardiac structure and function in the Fischer344×Brown Norway female rat. J Gerontol A Biol Sci Med Sci. 2016; 72:152–162. [PubMed: 27006078]

11. Wang H, da Silva J, Alencar A, et al. Mast cell inhibition attenuates cardiac remodeling and diastolic dysfunction in middle-aged, ovariectomized Fischer 344 × Brown Norway rats. J Cardiovasc Pharmacol. 2016; 68:49–57. [PubMed: 26981683]
12. Groban L, Yamaleyeva LM, Westwood BM, et al. Progressive diastolic dysfunction in the female mRen(2). Lewis rat: influence of salt and ovarian hormones J Gerontol A Biol Sci Med Sci. 2008; 63:3–11. [PubMed: 18245755]
13. Jessup JA, Wang H, MacNamara LM, et al. Estrogen therapy, independent of timing, improves cardiac structure and function in oophorectomized mRen2. Lewis rats Menopause. 2013; 20:860–868. [PubMed: 23481117]
14. Jessup JA, Zhang L, Chen AF, et al. Neuronal nitric oxide synthase inhibition improves diastolic function and reduces oxidative stress in ovariectomized mRen2. Lewis rats Menopause. 2011; 18:698–708. [PubMed: 21293310]
15. Jessup JA, Zhang L, Presley TD, et al. Tetrahydrobiopterin restores diastolic function and attenuates superoxide production in ovariectomized mRen2. Lewis rats Endocrinology. 2011; 152:2428–2436. [PubMed: 21427216]
16. Wang H, Jessup JA, Lin MS, Chagas C, Lindsey SH, Groban L. Activation of GPR30 attenuates diastolic dysfunction and left ventricle remodelling in oophorectomized mRen2. Lewis rats Cardiovasc Res. 2012; 94:96–104. [PubMed: 22328091]
17. Wang H, Jessup JA, Zhao Z, et al. Characterization of the cardiac renin angiotensin system in oophorectomized and estrogen-replete mRen2. Lewis rats PLoS One. 2013; 8:e76992. [PubMed: 24204720]
18. Ahmad S, Sun X, Lin M, et al. Blunting of estrogen modulation of cardiac cellular chymase/RAS activity and function in SHR. J Cell Physiol. 2018; 233:3330–3342. [PubMed: 28888034]
19. da Silva JS, Gabriel-Costa D, Wang H, et al. Blunting of cardioprotective actions of estrogen in female rodent heart linked to altered expression of cardiac tissue chymase and ACE2. J Renin Angiotensin Aldosterone Syst. 2017; 18:147032031772227.
20. Alencar AK, Montes GC, Montagnoli T, et al. Activation of GPER ameliorates experimental pulmonary hypertension in male rats. Eur J Pharm Sci. 2017; 97:208–217. [PubMed: 27836751]
21. Wang H, Zhao Z, Lin M, Groban L. Activation of GPR30 inhibits cardiac fibroblast proliferation. Mol Cell Biochem. 2015; 405:135–148. [PubMed: 25893735]
22. Zhao Z, Wang H, Lin M, Groban L. GPR30 decreases cardiac chymase/angiotensin II by inhibiting local mast cell number. Biochem Biophys Res Commun. 2015; 459:131–136. [PubMed: 25712524]
23. Wang H, Sun X, Chou J, et al. Cardiomyocyte-specific deletion of the G protein-coupled estrogen receptor (GPER) leads to left ventricular dysfunction and adverse remodeling: A sex-specific gene profiling analysis. Biochim Biophys Acta. 2017; 1863:1870–1882.
24. Dai D-F, Chiao Y, Marcinek DJ, Szeto HH, Rabinovitch PS. Mitochondrial oxidative stress in aging and healthspan. Longev Healthspan. 2014; 3:6. [PubMed: 24860647]
25. Doshi SB, Agarwal A. The role of oxidative stress in menopause. J Midlife Health. 2013; 4:140–146. [PubMed: 24672185]
26. Salini A, Jeyanthi GP. Impact of estradiol on circulating markers of oxidative stress among hypertensive postmenopausal women with comorbidities. Int J Med Res Rev. 2014; 2:544–552.
27. Colom B, Oliver J, Garcia-Palmer FJ. Sexual dimorphism in the alterations of cardiac muscle mitochondrial bioenergetics associated to the ageing process. J Gerontol Ser A Biol Sci Med Sci. 2015; 70:1360–1369. [PubMed: 24682352]
28. Lagranha CJ, Deschamps A, Aponte A, Steenbergen C, Murphy E. Sex differences in the phosphorylation of mitochondrial proteins result in reduced production of reactive oxygen species and cardioprotection in females. Circ Res. 2010; 106:1681–1691. [PubMed: 20413785]
29. Liu L, Kashyap S, Murphy B, et al. GPER activation ameliorates aortic remodeling induced by salt-sensitive hypertension. Am J Physiol Heart Circ Physiol. 2016; 310:H953–H961. [PubMed: 26873963]
30. Lindsey SH, Yamaleyeva LM, Brosnihan KB, Gallagher PE, Chappell MC. Estrogen receptor GPR30 reduces oxidative stress and proteinuria in the salt-sensitive female mRen2. Lewis rat Hypertension. 2011; 58:665–671. [PubMed: 21844484]

31. Liu S-B, Han J, Zhang N, Tian Z, Li X-B, Zhao M-G. Neuroprotective effects of oestrogen against oxidative toxicity through activation of G-protein-coupled receptor 30 receptor. Clin Exp Pharmacol Physiol. 2011; 38:577–585. [PubMed: 21645039]
32. De Francesco EM, Rocca C, Scavello F, et al. Protective role of GPER agonist G-1 on cardiotoxicity induced by doxorubicin. J Cell Physiol. 2017; 232:1640–1649. [PubMed: 27607345]
33. Murphy MP. Understanding and preventing mitochondrial oxidative damage. Biochem Soc Trans. 2016; 44:1219–1226. [PubMed: 27911703]
34. Adlam VJ, Harrison JC, Porteous CM, et al. Targeting an antioxidant to mitochondria decreases cardiac ischemia-reperfusion injury. FASEB J. 2005; 19:1088–1095. [PubMed: 15985532]
35. Graham D, Huynh NN, Hamilton CA, et al. Mitochondria-targeted antioxidant MitoQ10 improves endothelial function and attenuates cardiac hypertrophy. Hypertension. 2009; 54:322–328. [PubMed: 19581509]
36. Yancey DM, Guichard JL, Ahmed MI, et al. Cardiomyocyte mitochondrial oxidative stress and cytoskeletal breakdown in the heart with a primary volume overload. Am J Physiol Hear Circ Physiol. 2015; 308:H651–H663.
37. Ribeiro RF Jr, Dabkowski ER, Shekar KC, O Connell KA, Hecker PA, Murphy MP. MitoQ improves mitochondrial dysfunction in heart failure induced by pressure overload. Free Radic Biol Med. 2018; 117:18–29. [PubMed: 29421236]
38. Graziani M, Sarti P, Arese M, Magnifico MC, Badiani A, Saso L. Cardiovascular mitochondrial dysfunction induced by cocaine: Biomarkers and possible beneficial effects of modulators of oxidative stress. Oxid Med Cell Longev. 2017; 2017:3034245. [PubMed: 28593024]
39. Wang H, Sun X, Chou J, et al. Inflammatory and mitochondrial gene expression data in GPER-deficient cardiomyocytes from male and female mice. Data Brief. 2017; 10:465–473. [PubMed: 28054009]
40. Piao L, Choi J, Kwon G, Ha H. Endogenous catalase delays high-fat diet-induced liver injury in mice. Korean J Physiol Pharmacol. 2017; 21:317–325. [PubMed: 28461774]
41. Inafuku H, Kuniyoshi Y, Yamashiro S, et al. Determination of oxidative stress and cardiac dysfunction after ischemia/reperfusion injury in isolated rat hearts. Ann Thorac Cardiovasc Surg. 2013; 19:186–194. [PubMed: 22971810]
42. Rebrin I, Sohal RS. Pro-oxidant shift in glutathione redox state during aging. Adv Drug Deliv Rev. 2008; 60:1545–1552. [PubMed: 18652861]
43. Frijhoff J, Winyard PG, Zarkovic N, et al. Clinical relevance of biomarkers of oxidative stress. Antioxid Redox Signal. 2015; 23:1144–1170. [PubMed: 26415143]
44. Rebrin I, Kamzalov S, Sohal RS. Effects of age and caloric restriction on glutathione redox state in mice. Free Radic Biol Med. 2003; 35:626–635. [PubMed: 12957655]
45. Kelso GF, Porteous CM, Coulter CV, et al. Selective targeting of a redox-active ubiquinone to mitochondria within cells. J Biol Chem. 2001; 276:4588–4596. [PubMed: 11092892]
46. Smith RAJ, Kelso GF, Blaikie FH, et al. Using mitochondria-targeted molecules to study mitochondrial radical production and its consequences. Biochem Soc Trans. 2003; 31:1295–1299. [PubMed: 14641046]
47. James AM, Sharpley MS, Manas A-RB, et al. Interaction of the mitochondria-targeted antioxidant MitoQ with phospholipid bilayers and ubiquinone oxidoreductases. J Biol Chem. 2007; 282:14708–14718. [PubMed: 17369262]
48. Rodriguez-Cuenca S, Cochemé HM, Logan A, et al. Consequences of long-term oral administration of the mitochondria-targeted antioxidant MitoQ to wild-type mice. Free Radic Biol Med. 2010; 48:161–172. [PubMed: 19854266]
49. Zimmerman MA, Budish RA, Kashyap S, Lindsey SH. GPER-novel membrane oestrogen receptor. Clin Sci (Lond). 2016; 130:1005–1016. [PubMed: 27154744]
50. Graham D, Huynh NN, Hamilton CA, et al. Mitochondria-targeted antioxidant MitoQ10 improves endothelial function and attenuates cardiac hypertrophy. Hypertension. 2009; 54:322–328. [PubMed: 19581509]

51. McLachlan J, Beattie E, Murphy MP, et al. Combined therapeutic benefit of mitochondria-targeted antioxidant, MitoQ10, and angiotensin receptor blocker, losartan, on cardiovascular function. J Hypertens. 2014; 32:555–564. [PubMed: 24309493]
52. Gioscia-Ryan RA, Battson ML, Cuevas LM, Eng JS, Murphy MP, Seals DR. Mitochondria-targeted antioxidant therapy with MitoQ ameliorates aortic stiffening in old mice. J Appl Physiol. 1985; 2017:jap006702017. Epub ahead of print. doi: 10.1152/japplphysiol.00670.2017
53. Signorelli SS, Neri S, Sciacchitano S, et al. Behaviour of some indicators of oxidative stress in postmenopausal and fertile women. Maturitas. 2006; 53:77–82. [PubMed: 16325025]
54. Rossi R, Grimaldi T, Origliani G, Fantini G, Coppi F, Modena MG. Menopause and cardiovascular risk. Pathophysiol Haemost Thromb. 2002; 32:325–328. [PubMed: 13679667]
55. Dosi R, Bhatt N, Shah P, Patell R. Cardiovascular disease and menopause. J Clin Diagn Res. 2014; 8:62–64.
56. Rosano GMC, Vitale C, Marazzi G, Volterrani M. Menopause and cardiovascular disease: the evidence. Climacteric. 2007; 10(sup1):19–24. [PubMed: 17364594]
57. Jessup JA, Lindsey SH, Wang H, Chappell MC, Groban L. Attenuation of salt-induced cardiac remodeling and diastolic dysfunction by the GPER agonist G-1 in female mRen2. Lewis rats PLoS One. 2010; 5:e15433. [PubMed: 21082029]
58. Zapata-Sudo G, Alencar AK, Gabriel-Costa D, et al. Cardioprotection by activation of GPER in ovariectomized rats with pulmonary hypertension. Hypertension. 2016; 68:AP600.
59. Beral V, Bull D, Reeves G. Million Women Study Collaborators. Endometrial cancer and hormone-replacement therapy in the Million Women Study. Lancet. 2005; 365:1543–1551. [PubMed: 15866308]
60. Reel JR, Lamb JC IV, Neal BH. Survey and assessment of mammalian estrogen biological assays for hazard characterization. Fundam Appl Toxicol. 1996; 34:288–305. [PubMed: 8954758]
61. Bopassa JC, Eghbali M, Toro L, Stefani E. A novel estrogen receptor GPER inhibits mitochondria permeability transition pore opening and protects the heart against ischemia-reperfusion injury. Am J Physiol Heart Circ Physiol. 2010; 298:H16–H23. [PubMed: 19880667]
62. Sbert-Roig M, Bauzá-Thorbrügge M, Galmés-Pascual BM, et al. GPER mediates the effects of 17β-estradiol in cardiac mitochondrial biogenesis and function. Mol Cell Endocrinol. 2016; 420:116–124. [PubMed: 26628039]
63. Brown DA, Perry JB, Allen ME, et al. Expert consensus document: Mitochondrial function as a therapeutic target in heart failure. Nat Rev Cardiol. 2016; 14:238–250. [PubMed: 28004807]
64. Steagall RJ, Yao F, Shaikh SR, Abdel-Rahman AA. Estrogen receptor α activation enhances its cell surface localization and improves myocardial redox status in ovariectomized rats. Life Sci. 2017; 182:41–49. [PubMed: 28599865]
65. Kararigas G, Fliegner D, Forler S, et al. Comparative proteomic analysis reveals sex and estrogen receptor β effects in the pressure overloaded heart. J Proteome Res. 2014; 13:5829–5836. [PubMed: 25406860]
66. O'Lone R, Knorr K, Jaffe IZ, et al. Estrogen receptors α and β mediate distinct pathways of vascular gene expression, including genes involved in mitochondrial electron transport and generation of reactive oxygen species. Mol Endocrinol. 2007; 21:1281–1296. [PubMed: 17374850]
67. Meyer MR, Fredette NC, Daniel C, et al. Obligatory role for GPER in cardiovascular aging and disease. Sci Signal. 2016; 9:ra105. [PubMed: 27803283]
68. Liu X, Strable MS, Ntambi JM. Stearoyl CoA desaturase 1: Role in cellular inflammation and stress. Adv Nutr An Int Rev J. 2011; 2:15–22.
69. Wong SC, Fukuchi M, Melnyk P, Rodger I, Giaid A. Induction of cyclooxygenase-2 and activation of nuclear factor-kappaB in myocardium of patients with congestive heart failure. Circulation. 1998; 98:100–103. [PubMed: 9679714]
70. Montecucco F, Braunersreuther V, Lenglet S, et al. CC chemokine CCL5 plays a central role impacting infarct size and post-infarction heart failure in mice. Eur Heart J. 2012; 33:1964–1974. [PubMed: 21606075]
71. Sasagawa S, Nishimura Y, Okabe S, et al. Downregulation of GSTK1 is a common mechanism underlying hypertrophic cardiomyopathy. Front Pharmacol. 2016; 7:162. [PubMed: 27378925]

72. Brand MD, Esteves TC. Physiological functions of the mitochondrial uncoupling proteins UCP2 and UCP3. Cell Metab. 2005; 2:85–93. [PubMed: 16098826]

73. Han G, Li F, Yu X, White RE. GPER: A novel target for non-genomic estrogen action in the cardiovascular system. Pharmacol Res. 2013; 71:53–60. [PubMed: 23466742]

74. Pupo M, Maggiolini M, Musti AM. GPER mediates non-genomic effects of estrogen. Methods Mol Biol. 2016; 1366:471–488. [PubMed: 26585158]

75. Tamir S, Izrael S, Vaya J. The effect of oxidative stress on ERα and ERβ expression. J Steroid Biochem Mol Biol. 2002; 81:327–332. [PubMed: 12361722]

Background

Left ventricular diastolic dysfunction and hypertrophy are common correlates of female cardiac aging and precede heart failure with preserved systolic function. We previously reported that the newly identified G-protein coupled estrogen receptor (GPER) is involved in mediating estrogen's cardioprotective actions against pressure overload and aging. Here we show that GPER is a positive modulator of redox balance in the female heart and GPER deficiency in cardiomyocytes leads to increased oxidative stress which contributes to the development of left ventricular remodeling and dysfunction.

Translational Significance

Our findings suggest that the cardioprotective effects of GPER include an antioxidant role and that targeted strategies to limit oxidative stress after early noncancerous surgical removal of ovaries or menopause may help limit alterations in cardiac structure and function related to estrogen loss.

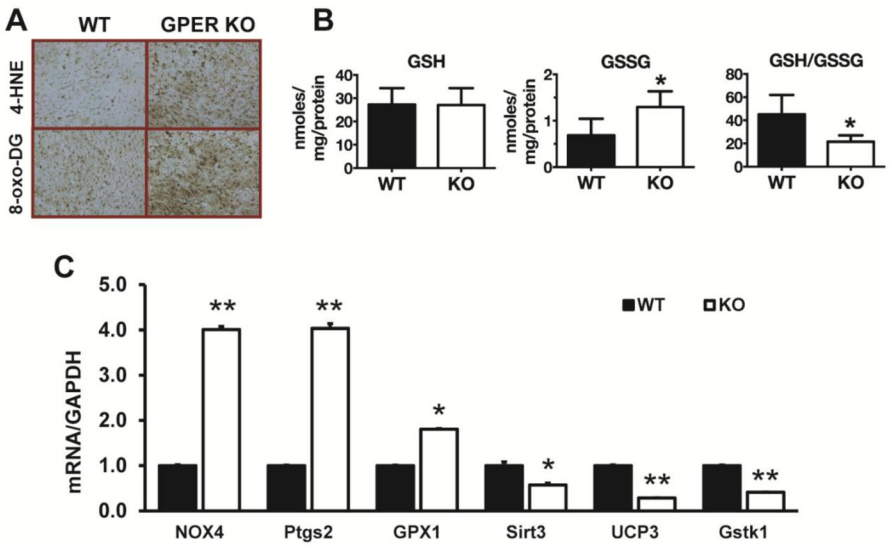

Figure 1. Cardiac oxidative stress in GPER KO mice

(A) Representative images of cardiac 4-HNE and 8-oxo-DG staining of LV from wild type (WT) and GPER knockout (KO) mice. **(B)** Cardiac GSH, GSSG, and the GSH/GSSG ratio in WT and GPER KO mice. Values are mean ± SEM. **P* < 0.05 vs WT. n = 5/group. **(C)** Cardiac mRNA levels of oxidative stress-related genes in WT and GPER KO mice. Values are mean ± SEM. **P* < 0.05, ***P* < 0.01 vs WT. n = 5/group.

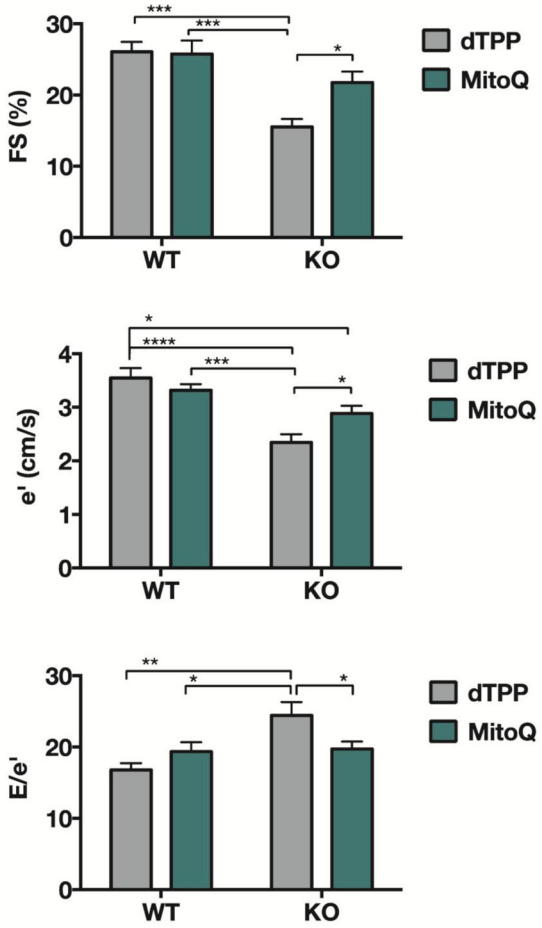

Figure 2. Echocardiographic measurements in WT and GPER KO mice treated with either MitoQ or dTPP

Data indicate percent FS (fractional shortening), e′ (early mitral annular velocity), and E/e′ (Doppler-derived filling pressure) in wild type (WT) and GPER KO (KO) mice. A two-way ANOVA was conducted to examine the effect of genotype and treatment and their interaction on each of these variables. Statistically significant interactions between genotype and treatment on FS [$F(1, 26) = 4.665$, $P = 0.041$], e′ [$F(1,26) = 6.650$, $P = 0.016$], and E/e′ [$F(1,26) = 7.335$, $P = 0.0123$] were observed. Post-hoc multiple comparisons showed that KO-dTPP mice had significantly reduced systolic function (reduced FS) and impaired diastolic function (reduced e′ and increased E/e′) when compared to WT mice treated with either dTPP or MitoQ, and to KO-MitoQ mice. There were no differences between WT mice treated with dTPP or MitoQ. Values are mean ± SEM. *$P < 0.05$; **$P < 0.01$; ***$P < 0.001$, ***$P < 0.0001$. n = 7–9/group.

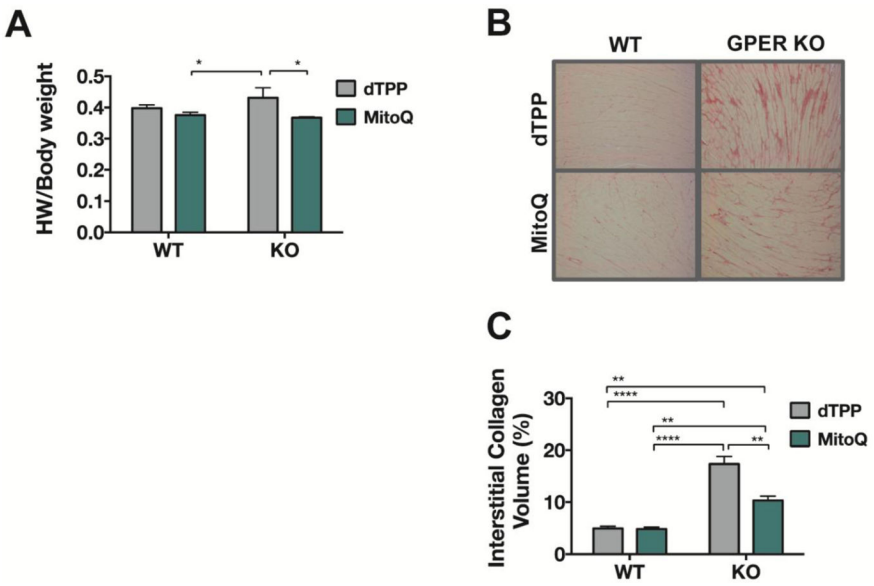

Figure 3. Heart weight and cardiac collagen deposition in WT and GPER KO mice treated with either MitoQ or dTPP

(A) Data represent heart weight (HW)-to-body weight ratio in WT and GPER KO mice treated with either MitoQ or dTPP control for 8 weeks. A two-way ANOVA was conducted to examine the effect of genotype and treatment on HW/body weight. There was a significant treatment effect [$F(1,26) = 6.52$, $P = 0.016$], with MitoQ significantly reducing HW normalized to body weight, specifically in KO mice ($P < 0.05$). While there was no overall difference in HW with respect to genotype [genotype effect: $F(1,26) = 0.468$], WT-MitoQ hearts normalized to body weight were lower when compared to KO-dTPP ($P < 0.05$). Values are mean ± SEM. *$P < 0.05$. n = 7–9/group. **(B)** Representative images of Picrosirius Red staining of LV tissue from WT and GPER KO mice treated with either MitoQ or dTPP. **(C)** Collagen deposition in the LV was quantified using ImageJ software. Two-way ANOVA revealed a significant genotype x treatment effect [$F(1,12) = 15.14$, $P = 0.002$], with collagen deposition in KO-MitoQ hearts significantly lower compared to KO-dTPP hearts ($P < 0.01$). As expected, the mitochondria-targeted antioxidant had no effect on interstitial collagen deposition in WT hearts, though WT hearts, irrespective of treatment, exhibited less collagen than KO-dTPP or KO-MitoQ. Values are mean ± SEM. **$P < 0.01$; ****$P < 0.0001$. n = 4/group.

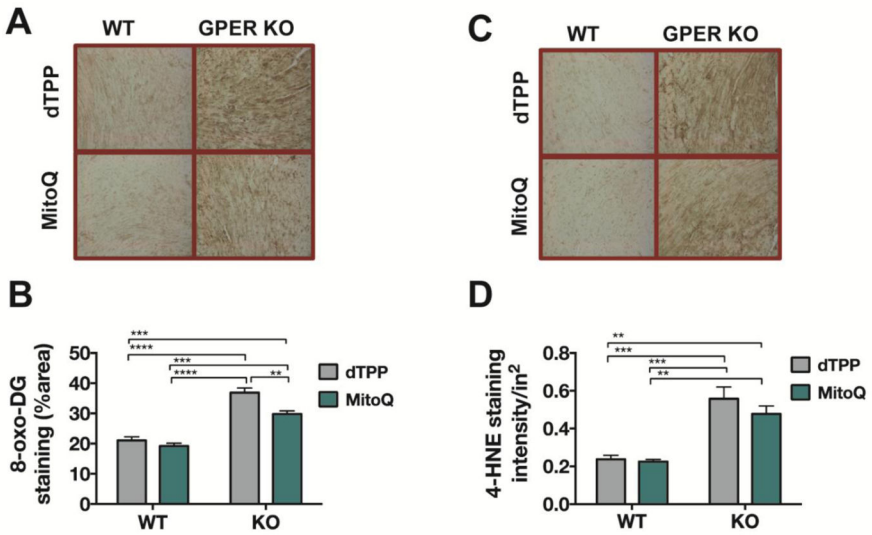

Figure 4. Cardiac 8-oxo-DG and 4-HNE staining in WT and GPER KO mice treated with either MitoQ or dTPP

(A,C) Representative images of cardiac 8-oxo-DG and 4-HNE staining from WT and GPER KO mice treated with either MitoQ or dTPP for 8 weeks. **(B, D)** Quantification of 8-oxo-DG and 4-HNE staining in the heart using ImageJ software. A two-way ANOVA was conducted to examine the effect of genotype and treatment on these measures of cardiac ROS. There were significant overall effects for genotype [$F(1,12) = 114$, $P < 0.0001$] and treatment [$F(1,12) = 13.20$, $P = 0.003$] on DNA damage, as reflected in 8-oxo-DG staining, whereas injury from lipid peroxidation, based on 4-HNE staining, revealed only a main effect of genotype [$F(1,12) = 51.80$, $P < 0.0001$]. Values are mean ± SEM. $^{**}P < 0.01$; $^{***}P < 0.001$, $^{****}P < 0.0001$; n = 4/group.

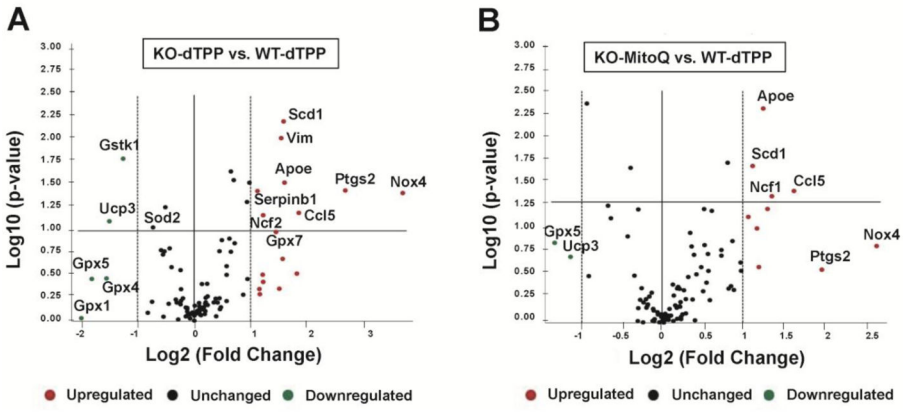

Figure 5. Volcano plot representing real-time RT-PCR microarray analysis

Expression of 84 genes associated with oxidative stress were analyzed in the LV of GPER KO and WT mice treated with either MitoQ or dTPP. The graphs summarize fold-change and *t*-test criteria. The x-axis represents fold difference (Log2) in expression in GPER KO mice compared to WT mice receiving either MitoQ or the inactive compound dTPP. The y-axis represents the *P*-value (Log10). The center vertical line indicates a fold-change in gene expression of 1. The other two vertical lines indicate a threshold of two-fold changes in gene expression. The horizontal line indicates a threshold of $P = 0.05$. **(A)** Volcano plot of upregulated, downregulated, and unchanged oxidative stress genes in LV from GPER KO versus WT mice treated with dTPP (n = 3/group). **(B)** Volcano plot of upregulated, downregulated, and unchanged oxidative stress genes in LV from GPER KO mice treated with MitoQ versus WT mice treated with dTPP.

Table 1

Body Weight, Blood Pressure and Echocardiographic Indices of Left Ventricular Structure and Function

	dTPP Mean ± SEM	MitoQ Mean ± SEM	Treatment *P*-value	Genotype *P*-value	Treatment × Genotype *P*-value
Body weight (gm)					
Wild type	27.2 ± 0.8	28.3 ± 1.3	0.144	0.091	0.756
GPER KO	28.5 ± 0.6	30.3 ± 1.0			
SBP (mmHg)					
Wild type	99 ± 2	102 ± 4	0.982	0.411	0.444
GPER KO	99 ± 4	96 ± 3			
LVEDD (mm)					
Wild type	3.8 ± 0.1	3.6 ± 0.1	0.314	0.948	0.508
GPER KO	3.7 ± 0.1	3.7 ± 0.1			
LVESD (mm)					
Wild type	2.8 ± 0.1	2.7 ± 0.1	0.136	0.029	0.636
GPER KO	3.2 ± 0.2	2.9 ± 0.1			
PWTed (mm)					
Wild type	0.83 ± 0.04	0.88 ± 0.05	0.856	0.971	0.246
GPER KO	0.89 ± 0.06	0.82 ± 0.04			
AWTed (mm)					
Wild type	0.95 ± 0.05	0.85 ± 0.05	0.125	0.753	0.510
GPER KO	0.91 ± 0.05	0.87 ± 0.01			
RWT					
Wild type	0.44 ± 0.03	0.48 ± 0.03	0.256	0.255	0.263
GPER KO	0.50 ± 0.05	0.43 ± 0.02			
Emax (cm/s)					
Wild type	59 ± 2	67 ± 5	0.272	0.103	0.308
GPER KO	56 ± 4	57 ± 3			

	dTPP Mean ± SEM	MitoQ Mean ± SEM	Treatment *P*-value	Genotype *P*-value	Treatment × Genotype *P*-value
E dec time (msec)					
Wild type	32 ± 4	34 ± 3	0.413	**0.001**	0.819
GPER KO	21 ± 2	24 ± 3			
Heart Rate (bpm)					
Wild type	433 ± 26	459 ± 18	0.799	0.370	0.376
GPER KO	473 ± 26	459 ± 17			

Notes: SBP, systolic blood pressure; LV, left ventricular; LVEDD, left ventricular end diastolic dimension; LVESD, left ventricular end systolic dimension; PWTed, posterior wall thickness end diastole; AWTed, anterior wall thickness end diastole; RWT, relative wall thickness; Emax, Early transmitral filling velocity; E dec time, early deceleration time; cm/s, centimeters per second; mm, millimeters; mmHg, millimeters of mercury; dTPP, inactive comparison compound decylTPP; MitoQ, MitoQuinone. The groups consisted of Wild type-dTPP (N= 7), GPER KO-dTPP (N= 7), Wild type-MitoQ (N= 7), GPER KO-MitoQ (N=9). Using a two-way ANOVA, significant differences in body weight, systolic blood pressure, LV structure and function, with respect to treatment (dTPP vs. MitoQ), genotype (wild-type vs. GPER KO), and treatment x genotype, were determined. p values are presented on the right of the table. For convenience, significant differences are indicated in bold.